Nanoscale

Accepted Manuscript

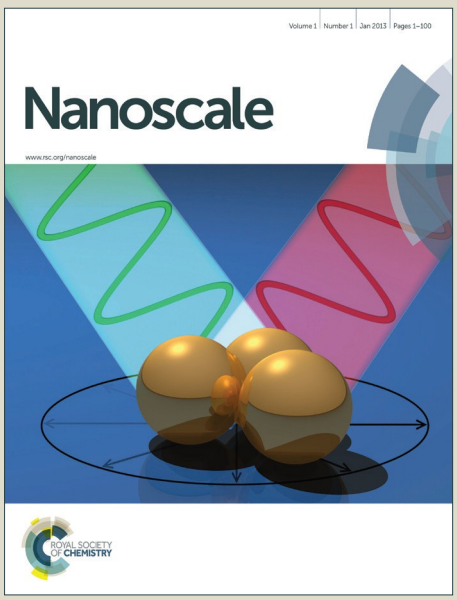

ROYAL SOCIETY OF CHEMISTRY

www.rsc.org/nanoscale

Cite this: DOI: 10.1039/c0xx00000x

www.rsc.org/xxxxxx

ARTICLE TYPE

Metal Complex Modified Azo Polymer for Multilevel Organic Memories

Yong Ma[a], Hong-Xia Chen[a], Feng Zhou[a], Hua Li[a], Huilong Dong[c], You-Yong Li[b, c], Zhi-Jun Hu[b, d] Qing-Feng Xu [a, b]* and Jian-Mei Lu [a, b]*

Received (in XXX, XXX) XthXXXXXXXXX 20XX, Accepted Xth XXXXXXXXX 20XX

DOI: 10.1039/b000000x

Multilevel organic memories have attracted considerable interest due to their high capacity of data storage. Despite advances, the search of multilevel memory materials still remains a formidable challenge. Herein, we present a rational design and synthesis of a class of polymers containing azobenzene-pyridine group (PAzo-py) and its derivatives, for multilevel organic memory storage. In this design, metal complex (M(Phen)Cl_2, M= Cu, Pd) is employed to modify the HOMO-LUMO energy levels of azo polymer, thereby converting the memory states from binary to ternary. More importantly, this approach enables modulating the energy levels of azo polymers by varying the coordination metal ions. This makes the achievement of high performance multilevel memory performance possible. The ability to tune the bandgap energy of azo polymers provides new exciting opportunities to develop new materials for high-density data storage.

Introduction

Organic materials are expected to be widely used in the next generation of electronic systems such as logic circuits, radio frequency (RF) identification tags, organic light emitting diodes (OLEDs), solar cells, and others.[1-6] Memory is an essential part of electronic systems, used for data processing, storage, and communication. However, currently available inorganic memories are not compatible with the flexible organic electronics used for next generation high density data storage.[7-10] In the design of non-volatile memory devices, polymer materials are excellent candidates as active layers for large-area electronic devices. Due to their printability, polymers display excellent solution processibility and high-throughput fabrication, thus making them ideal for this function[11-14] A lot of research on polymer memory devices have focused on binary data storage with thermal, electronic or optical bistable polymers.[15-17] Tremendous effort has been made to develop various materials and improve the memory performance of device parameters such as low open voltage, large memory window and storage capacity.[18, 19] The ability to store multi-bit information provides an effective way to increase the memory density per unit cell area. Compared with binary counterparts, multilevel memories are much more challenging because suitable materials are not accessible and the underlying mechanisms are controversial.[20] Lots of multilevel memories rely on small molecules with D-A structure, which are found in organometallics with two or more reversible oxidation states.[21] However, polymer-based memories offer several advantages such as solution processing and higher structural diversity.[22, 23] The strategy presented here is to combine a single polymer displaying binary memory performance with a metal complex that has strong charge transfer effect; this combination results in ternary performance. Generally, under an electric field, the transition of electrons from the highest occupied molecular orbital (HOMO) to lowest unoccupied molecular orbital (LUMO) energy level causes the device to switch from OFF state to ON state, indicating a data 'writing' process. If a new electron transition channel (new HOMO-LUMO bandgap energy) is introduced, a new conduction state can be anticipated. In polymeric complex based devices, two different electron transition channels exist when ternary memory behaviour shows. Herein, we report a homopolymer (PAzo-py) with a stable WORM memory performance. After a metal complex ($Cu(Phen)Cl_2$ or $Pd(Phen)Cl_2$) was employed to form a polymeric complex, the polymeric complex based device ITO(Au)/PAzo-py-$Cu(Phen)Cl_2$/Al(Au) exhibited a ternary memory performance (**Figure 1**). Its memory mechanism was attributed to the differentiation degree of HOMO-LUMO energy levels in a single polymer system, in which the charge transfer (CT) process of the metal centre and surrounding ligands created a new bandgap energy while the original electron transition (charge traps) of Azo counterpart was preserved.

Experimental

Materials

4-Aminopyridine (98%, Aldrich), phenol (99%, Fluka), methacryloyl chloride (97%, Fluka), 1,10-phenanthroline(99%, Aldrich), $CuCl_2 \cdot 2H_2O$ were purchased and used directly without further purification. Azoisobutyronitrile (AIBN) was purchased from Aldrich and recrystallized from methanol prior to use.

Dimethylformamide (DMF), cyclohexanone, and tetrahydrofuran (THF) were distilled under an inert atmosphere prior to use.

Apparatus

Instrumentation and Characterizations: ^{1}H NMR spectra were measured on an INOVA 400 MHz FT-NMR spectrometer, using $CDCl_3$ or DMSO-d_6 as solvent and tetramethylsilane (TMS) as the internal standard at ambient temperature. The UV-vis absorption spectra were recorded on a Perkin Elmer Lambda-17 spectrophotometer at room temperature. Weight-average (M_w) and number-average molecular weight (M_n) was determined by gel permeation chromatography (GPC) on Waters1515 Gel Chromatograph with tetrahydrofuran (THF) as the solvent. Monodisperse polystyrene samples were used as the standard. Elemental analysis of C, H and N was performed by the Elemental Analysis Service using an EA1110-CHNS elemental analyzer. Infrared spectra were measured as KBr disks on a MagNa-550 FT-IR system. Cyclic voltammetry (CV) measurements were carried out in 0.1 M DMF solution of tetra-n-butyl-ammonium hexafluorophosphate ($TBAPF_6$) using a CHI-660C electrochemical workstation with a platinum gauze auxiliary electrode and an Ag/AgCl reference electrode. The devices were characterized at room temperature under ambient conditions, using an Agilent Technologies B1500A Semiconductor device Analyzer. SEM images were taken on a Hitachi S-4700 scanning electron microscope. X-Ray Photoelectron Spectroscopy (XPS) analyses were performed on a Thermo K-Alpha photoelectron spectrometer. Atomic force microscopy (AFM) measurements were performed using a MFP-3DTM (Digital Instruments/Asylum Research) AFM instrument. The copper content was measured by means of inductively coupled plasma atomic emission spectroscopy (ICP-AES, Thermo Elemental IRIS 1000) using HCl/HNO_3 digestion.

Synthesis and characterization of PAzo-py and PAzo-py-Cu(Phen)Cl_2 and Pyvp.

Synthesis of 4-((4-methacryloyloxy)-phenylazo)pyridine (Azo-py) and Cu(Phen)Cl_2 was prepared by the method described earlier.[24,25]

Pink powders of Azo-py with good yield (67%) were obtained. ^{1}H NMR($CDCl_3$): δ (ppm)= 8.80 (d, *J* =4.8 Hz, 2H, Ar-H), 8.01 (d, *J*= 8.8 Hz, 2H, Ar-H), 7.69 (d, *J*= 4.8 Hz, 2H, Ar-H), 7.31 (d, *J*= 8.8 Hz, 2H, Ar-H), 6.39 (s, 1H, CH_2 = C-), 5.81 (s, 1H, CH_2 = C-), 2.08 (s, 3H, -CH_3). IR(KBr, cm^{-1}): 3433(b), 1715(s), 1633(m), 1563(m), 1493(m), 1400(m), 1283(m), 1212(s), 1131(s), 990(m), 944(w), 897(m), 827(m), 546(s). Anal. Calc. For $C_{15}H_{13}N_3O_2$(%): C 67.40, H 4.90, N 17.96; Found: C 67.48, H 5.01, N 17.90%.

Synthesis of PAzo-py.

PAzo-py was synthesized via free radical polymerization: 100 mmol (2.67g) of the corresponding monomer (Azo-py) and 10 mmol of AIBN (16.4mg) were added to 25 mL of freshly distilled cyclohexanone in a Schlenk tube. The reaction mixture was deoxygenated by freeze-pump-thawing and backfilling with Ar (three times). The polymerization was carried out at 90°C over 18 h under Ar atmosphere. The reaction mixture was poured into 500 mL of methanol, and 100~150 mL of 2% aqueous NaOH was added to the resulting mixture. The mixture was cooled in the freezer overnight. The resulting polymeric solid was filtered off and thoroughly washed with methanol and hexane. Finally, the polymer was dried at 60°C under vacuum. PAzo-py: Yield: 57%. ^{1}H NMR ($CDCl_3$): δ=1.0-2.1 (m, 5H), 7.0-7.3 (m, 2H), 7.3-7.7(m, 2H), 7.7-8.1 (m, 2H), 8.4-8.9 (m, 2H). IR (KBr): 3423(b), 3033(b), 1751(s), 1589(s), 1494(m), 1195(s), 1101(s), 833(m), 561(w). Anal. Calc. For $(C_{15}H_{13}O_2N_3)_n$ $(267.3)_n$: C 67.40, H 4.90, N 17.96; Found: C 67.10, H 5.15, N 17.80%. Synthesis of Pyvp was followed the above way and the characterization is provided in the supporting information.

Synthesis of PAzo-py-Cu(Phen)Cl_2.

PAzo-py (20mg, 2.17mmol) and Cu(Phen)Cl_2 (4mg, 12.7mmol) were dissolved in 2.5 mL dimethylformamide (DMF), and the reaction mixture was gently heated to 75°C under stirring for 3 h. The insoluble portion was subsequently removed.

Fabrication of memory devices

Fabrication and characterization of ITO/polymer/Al or Au sandwich device: The indium-tin-oxide (ITO) glass substrate was precleaned sequentially with water, acetone, and alcohol in an ultrasonic bath for 20 min. The active film was spin-coated onto the ITO-glass substrate at a rotational speed of 2000 rpm for 40 s. The film thickness was determined by SEM cross-section. The metal of Al or Au, with thicknesses of approximately 65 nm, was thermally evaporated and deposited onto the organic surface at approximately 5×10^{-6} Torr through a shadow mask to form the top electrode. An active device area of approximately 0.0314 mm^2 was obtained. All electrical measurements of the device were characterized using an Agilent Technologies B1500A Semiconductor device Analyzer under ambient conditions, without encapsulation,.

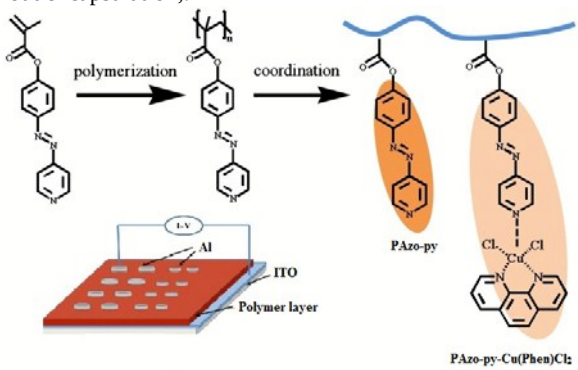

Figure 1. Synthetic routine of PAzo-py and PAzo-py-Cu(Phen)Cl_2.

Results and discussion

Preparation and characterization of polymer and polymeric complex

Poly(4-((4-methacryloyloxy)-phenylazo)pyridine)(PAzo-py) was confirmed by ^{1}H NMR (**Figure S1**), TGA-DSC and GPC. Its metal complexes PAzo-py-Cu(Phen)Cl_2 was confirmed by TGA-DSC, EDS (**Figure S3a**), XRD (**Figure S3b**) and Elemental Analysis. The number-average molecular weight (M_n) of PAzo-py is 9200 with a polydispersity index (PDI) of 1.55, in which the

average amount of the azobenzene unit is around 35 in a single chain. As shown in the TGA curves (**Figure S2**), the thermal decomposition temperature (the 5% weight-lost temperature) of polymer and polymeric complex were higher than 250 ^{o}C. Good thermal stability endures heat deterioration in the memory devices. The UV–Vis absorption spectrum of PAzo-py film exhibited one major absorption peak between 260 nm and 380 nm arise from the π–π* transition of azobenzene groups (**Figure S4**). The UV-vis spectra of PAzo-py-M(Phen)Cl_2 films show a main absorption band (325 nm) with a shoulder at 230 nm, assigned to π-π transition of phen group. However, the UV spectra pattern slightly broadens after 450 nm, indicating the charge transfer process of Cu(II) and the pyridine group.[26,27] The atomic force microscopy (AFM) measurements of devices showed 2.39 nm for roughness of PAzo-py film, 3.16 nm for roughness of PAzo-py-Cu(Phen)Cl_2 film, 3.09 nm for roughness of PAzo-py-Pd(Phen)Cl_2 film (**Figure S5)**. The small surface roughness of the films leads to the good quality of the films, which indicates the likeliness of high performance devices.

Memory performances

Sandwich memory devices with an active layer of PAzo-py, PAzo-py-Cu(Phen)Cl_2 and PAzo-py-Pd(Phen)Cl_2 were prepared using ITO and Al as bottom and top electrodes, respectively.[28,29] The I-V characteristic of PAzo-py-based device depicts an abrupt increase in current from 10^{-5} A to 10^{-2} A (sweep 1) at a threshold voltage of approximately -4.0 V, as shown in **Figure 2a**. The high-conductivity observed during the subsequent voltage sweep (sweep 2) showed retention of the ON state, revealing the nonvolatile characteristic of the device. Furthermore, the polymer Pyvp has same structure of PAzo-py, except without azo-group; its incorporation into the memory device showed no obvious memory performance (**Figure S6**). This verifies that the azobenzene group plays an important role in the memory performance.

Upon coordination, the polymeric complex-based device showed interesting multilevel memory performance. As shown in **Figure 2b,** the device ITO/PAzo-py-Cu(Phen)Cl_2/Al remained in a low-conductivity (OFF) state when a voltage sweep was initially applied. It switched to the intermediate-conductivity (ON1) state at a threshold voltage of approximately -1.8 V, as indicated by the abrupt increase of the current from 10^{-7} A to 10^{-5} A (sweep 1, "writing" process). The subsequent voltage sweep (sweep 2) indicated that the device retained the ON1 state (the intermediate state). When the maximum of the negative bias was set even higher (sweep 3 from 0 to -6.0 V), the current increased from 10^{-5} A to 10^{-2} A at a threshold voltage of -3.5 V. The device remained well in the high conductivity state during the subsequent fourth sweep (from 0 to -6.0 V) and the reverse fifth sweep (from 0 to 6.0 V). At a constant stress of -1.0 V, no obvious degradation in the current was observed for the ON1, ON2 and OFF states during the long-term testing of about 10^4 s (**Figure 2c, d)**. The WORM memory type preserves well in the polymeric complex system.

The effect of film thickness (105 and 48 nm) on the memory performances of the PAzo-py-Cu(Phen)Cl_2 device was also studied (**Figure 3a, b**). As the film thickness increased to 105 nm, the turn-on voltage increased to -1.9 V and -3.8 V from -1.8 V and -3.5 V, respectively. While as the film thickness decreased to 48 nm, no obvious changes happened to the turn-on voltage. Ternary performance was observed in these devices with a slight change in switching voltage. Furthermore, as the content of Cu^{2+} in PAzo-py-Cu(Phen)Cl_2 complexes were adjusted from 2% to 3%, ternary performance was also observed. However, as the content continued to increase, phase separation occurred more easily, making Cu^{2+} increase detrimental stability of the device. Taken together, these data clearly indicated that the PAzo-py-Cu(Phen)Cl_2 based memory devices possessed good stability and reproducibility.

To compare the interfacial effect of different electrodes and organic film, symmetric Au electrodes were used to prepare the Au/PAzo-py/Au and Au/PAzo-py-Cu(Phen)Cl_2/Au devices. The WORM binary performance was observed in a Au/PAzo-py/Au device with a switching voltage of -1.5V and ON/OFF ratio of about 10^7 when a bias voltage was applied (**Figure S8**). For the device with Au/polymer complex/Au, the ternary memory performance was observed with two switching voltages at -1.1V and -2.5V, and when the ON/OFF ratios at 10^3 and 10^2, respectively (**Figure 3c**). Compared to those of ITO/polymer/Al devices, the switching voltages all reduced significantly, with a higher ON/OFF ratio obtained. This can be partly attributed to the lower bandgap energy due to the lower work function of the Au electrode (-5.1 eV) than that of the Al electrode (-4.8 eV). However, the Au electrodes only reduce the switching voltage and improve the ON/OFF ratio without changing the binary performance to ternary performance. Most likely, the ternary performance originates from the material itself.

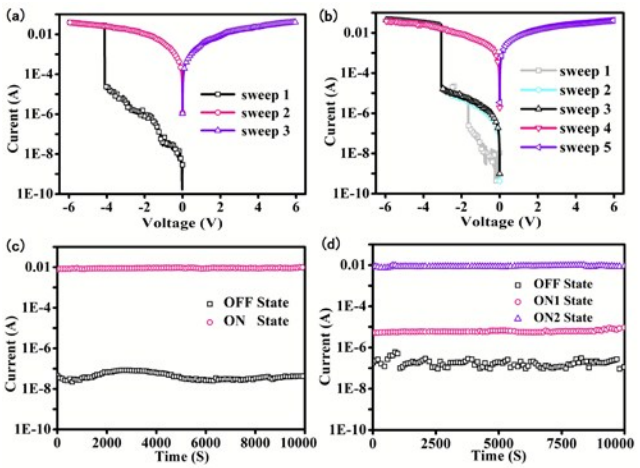

Figure 2. Current-voltage (I-V) characteristics of the memory device ITO/PAzo-py/Al (a) and ITO/PAzo-py-Cu(Phen)Cl_2/Al (b); Stability of the device ITO/PAzo-py/Al (c) and ITO/PAzo-py-Cu(Phen)Cl_2/Al (d) under a constant voltage of -1.0 V.

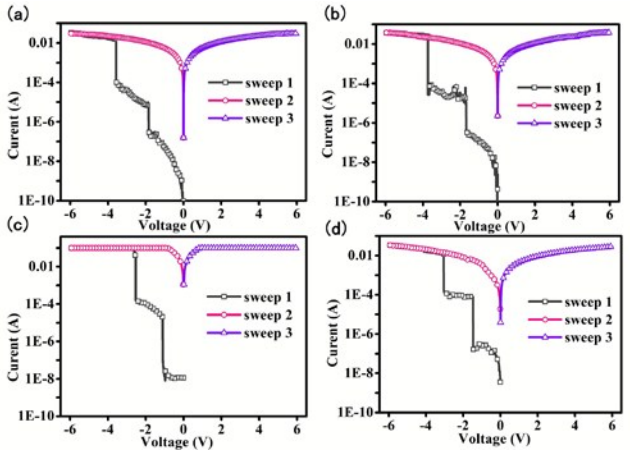

Figure 3. Current-voltage (I-V) characteristics of the memory device ITO/PAzo-py-Cu(Phen)Cl_2(105nm)/Al (a), ITO/PAzo-py-Cu(Phen)Cl_2 (48nm)/Al (b), Au/PAzo-py-Cu(Phen)Cl_2/Au (c), ITO/PAzo-py-Pd(Phen)Cl_2/Al (d).

Additionally, the I-V characteristic measurement of Pd-based devices confirmed the presence of ternary performance with switching voltages at -1.4 and -3.0 V (**Figure 3d**). As the band gap energy of PAzo-py-Pd(Phen)Cl_2 (0.39 eV) became lower than PAzo-py-Cu(Phen)Cl_2 (which is affected by the stronger coordination ability of Pd), the turn-on voltage of device ITO/PAzo-py-Pd(Phen)Cl_2/Al-based device was also lower than that of the ITO/PAzo-py-Cu(Phen)Cl_2/Al-based device. This indicated the feasibility and effectiveness of this strategy for ternary memory materials.

Mechanisms

Table 1. The DFT results: HOMO, LUMO, ESP and EB of Azo-py, Azo-py-Cu(Phen)Cl_2 and Azo-py-Pd(Phen)Cl_2.

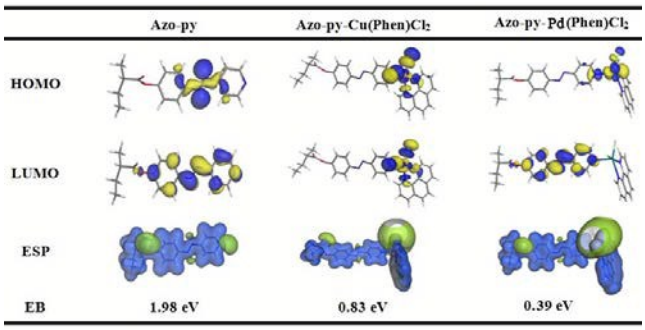

Theoretical calculations of moiety Azo-py and its metal complex Azo-py-M(Phen)Cl_2 (M = Cu, Pd) were listed in **Table 1** and detailed information was provided in Supporting Information. According to the Density Functional Theory (DFT) calculation, the Azo-py group contained numerous negative electrostatic potential (ESP) zones (yellow) that form charge traps due to the azo structure and pyridyl group. The bandgap energy between the HOMO and LUMO energy levels of Azo-py was 1.98 eV. However, upon coordinating with Cu(Phen)Cl_2 or Pd(Phen)Cl_2, the negative ESP zone of Azo-py-Cu(Phen)Cl_2 and Azo-py-Pd(Phen)Cl_2 decreased. According to calculation results, the bandgap energy of Azo-py-Cu(Phen)Cl_2 and Azo-py-Pd(Phen)Cl_2 were 0.83 eV and 0.39 eV; these values were distinctly different from that of Azo-py itself. Both uncoordinated and coordinated Azo-py moieties were present in the obtained polymeric metal complex, indicating the formation of two types of electron transition tunnels.

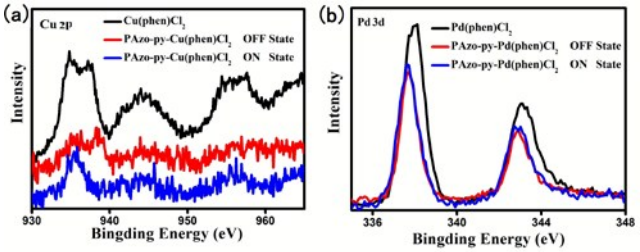

Figure 4. XPS spectra of Cu 2p for PAzo-py-Cu(Phen)Cl_2 film (a) and Pd 3d for PAzo-py-Pd(Phen)Cl_2 film (b) in devices. The ON state means the film after the voltage applied with mercury drop as the top electrode.

Further experimentation was conducted to investigate the origin of the ternary performance. Several characterizations were performed before and after voltage was applied on the polymer film; the characterizations include diffusion reflectance UV-vis spectra, XPS and CV measurements.

According to the results of UV-vis spectra, at around 300 nm, the broad absorption band of PAzo-py based device narrowed and red-shifted after the electrical field was applied, and did not recover even after several days. Similar results were obtained from the PAzo-py-Cu(Phen)Cl_2 based device and this illustrated the nonvolatile property of these polymer devices.

From XPS results, shown in **Figure 4a**, a peak located at 933.6 eV, with two satellite peaks at 944.0 and 941.2 eV, were assigned to Cu $2p^{3/2}$ for Cu(II). The XPS measurement of Cu $2p^{3/2}$ for ON state and OFF state of PAzo-py-Cu(Phen)Cl_2 film showed that there were no significant changes comparing to Cu(Phen)Cl_2 complex (**Figure 4a)**. The ON state of the device meant that voltage had been applied to the film with a mercury drop top electrode until ON state was reached. The ON state also showed peaks at 933.8 eV and 944.2 eV, assigned to Cu $2p^{3/2}$. This suggested that the Cu(Phen)Cl_2 complex stabilized after coordination with the pyridine group. The XPS measurement of Pd element for PAzo-py-Pd(Phen)Cl_2 film also showed the similar results (**Figure 4b**). Therefore, redox reaction of center metal ions during the conduction process can be excluded from consideration.

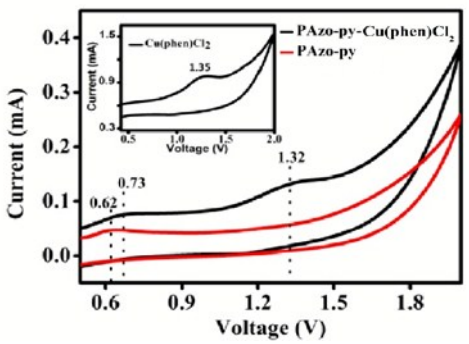

Figure 5. Cyclic voltammetry (CV) of PAzo-py and PAzo-py-Cu(Phen)Cl_2 with 0.1 M $TBAPF_6$ in DMF solution. The scan rate: 100 mV s^{-1}. The figure inserted showed the CV measurement of Cu(Phen)Cl_2.

As shown in **Figure 5**, the cyclic voltammetry measurement result indicates that PAzo-py-Cu(Phen)Cl_2 film possesses two oxidation peaks (0.73 and 1.32 V) corresponding to the PAzo-py (0.62 V) and the Cu(Phen)Cl_2 complex (1.35 V), respectively; this reveals the presence of two oxidation states in the polymeric complex matrix. Therefore, the ternary memory performance can be explained by two factors: the electron transition of the polymer itself and new electron transition due to the formation of metal-ligand charge transfer.

Therefore, the mechanism of PAzo-py based memory is mainly attributed to the azobenzene moieties which can serve as "traps" to impede the mobility of charge carriers.[30] When bias voltage is applied, electrons in the ground state transit from HOMO to LUMO; the traps located at the polymer side chain were gradually filled by charges and the device finally switches from low conductivity to high conductivity. The PAzo-py-Cu(Phen)Cl_2-based device's mechanism can be explained as follows: when the electric field is applied, charge generation occurs around the anode, accompanied by hole injection from the ITO to the polymeric complex. Under a continuously increasing electric field, electrons flow from the electron donor Azo-py to the electron accepter Cu(II) ions to form a filed induced charge transfer (CT) complex, resulting in the first abrupt current increase(i.e. from OFF state to ON1 state). The stable CT complex isn't easily dissociated even after the power was turned off or under non-degrading reverse voltage, indicating the new conductivity state is permanently maintained. As voltage continues to increase, more electrons can be transferred from the HOMO to LUMO level of the original Azo-py moiety, producing the second current spike. Consequently, a high conductivity state of the device is reached (i.e. ON1 state to ON2 state).

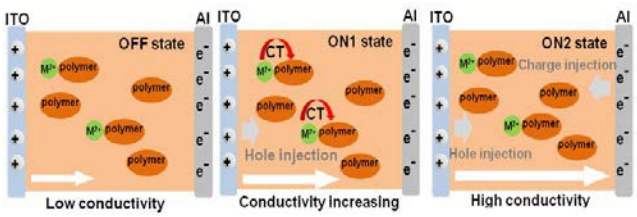

Figure 6. Conductive process for the device after applying the voltage.

Conclusion

In summary, polymeric metal complex-based devices exhibit interesting ternary performance while pure polymers only shows binary performance. According to calculations, the HOMO-LUMO bandgap energy can be tuned by the formation of polymeric complexes; tuning the bandgap energy affects the memory performance of materials. Two different kinds of electron transition tunnel appear in the same matrix, which may produce multistate memory property. This method provides the possibility of a much-needed solution to the preparation of materials with ternary or even higher multilevel storage performance. The results of this study hold great significance for the development of high-density data storage technology.

Acknowledgements

The authors graciously thank Prof. Qing-Hua Xu from National University of Singapore for helpful discussion. The authors graciously thank the Chinese Natural Science Foundation (21371128 and 21336005), Chinese-Singapore Joint Project (2012DFG41900), and Qing-Lan Project of Jiangsu Province

Notes and references

[a] Key Laboratory of Organic Synthesis of Jiangsu Province, School of Chemistry, Chemical Engineering and Materials Science, Soochow University (DuShuHu Campus), 199 Ren'ai Road, Suzhou, 215123, China
[b] Collaborative Innovation Center of Suzhou Nano Science and Technology, Soochow University, Suzhou 215123, China. E-mail: lujm@suda.edu.cn
[c] Jiangsu Key Laboratory of Carbon-Based Functional Materials & Devices, Institute of Functional Nano & Soft Materials (FUNSOM), Soochow University (DuShuHu Campus), 199 Ren'ai Road, Suzhou, 215123, China
[d] College of Physics, Optoelectronics and Energy, Soochow University, Suzhou, Jiangsu 215123, China

1 Giri, G.; Verploegen, E.; Mannsfeld, S. C. B.; Atahan-Evrenk, S.; Kim, D. H.; Lee, S. Y.; Becerril, H. A.; Aspuru-Guzik, A.; Toney, M. F.; Bao, Z. *Nature*. 2011, **480**, 504-508.
2 Lin, Y.; Li, Y.; Zhan, X. *Chem. Soc. Rev.* 2012, **41**, 4245-4272.
3 Xiao, J.; Yang, B.; Wong, J. I.; Liu, Y.; Wei, F.; Tan, K. J.; Teng, X.; Wu, Y.; Huang, L.; Kloc, C.; Boey, F.; Ma, J.; Zhang, H.; Yang, H. Y. and Zhang, Q. *Org. Lett.* 2011, **13**, 3004-3007.
4 Gu, P. Y.; Zhou, F.; Gao, J.; Li, G.; Wang, C.; Xu, Q. F.; Zhang, Q. and Lu, J. M. *J. Am. Chem. Soc.* 2013, **135**, 14086-14089.
5 Li, G.; Zheng, K.; Wang, C.; Leck, K. S.; Hu, F.; Sun, X. W. and Zhang, Q. *ACS Applied Materials & Interfaces*, 2013, **5**, 6458-6462.
6 Hu, B.; Wang, C.; Wang, J.; Gao, J.; Wang, K.; Wu, J.; Zhang, G.; Cheng, W.; Venkateswarlu, B.; Wang, M.; Lee, P. S. and Zhang, Q. *Chemical Science*, 2014, **5**, 3404-3408.
7 Hu, B. L.; Zhu, X. J.; Chen, X. X.; Pan, L.; Peng, S. S.; Wu, Y. Z.; Shang, J.; Liu, G.; Yan, Q. and Li, R. W. *J. Am. Chem. Soc.* 2012, **134**, 17408−17411.
8 Zhang, L.; Li, M.; Wang, Y.; Yin,Q. Z.; Zhang, W. *SCIENTIFIC REPORTS*, 2013, **3**, 2487-2498.
9 Khan, M. A.; Caraveo-Frescas, J. A.; Alshareef, H. N. *Organic Electronics*, 2015, **16**, 9-17.
10 You, Y.; Yang, K.; Yuan, S.; Dong, S.; Zhang, H.; Huang, Q.; Gillin, W. P.; Zhan, Y.; Zheng, L. *Organic Electronics*, 2014, **15**, 1983-1989.
11 Baek, S.; Lee, D.; Kim, J.; Hong, S. H.; Kim, O.; Ree, M. *Adv. Funct. Mater.* 2007, **17**, 2637-2644.
12 Hahm, S.; Choi, S.; Hong, S. H.; Lee, T.; Park, S.; Kim, D.; Kwon, W. S.; Kim, K.; Kim, O.; Ree, M. *Adv. Funct. Mater.* 2008, **18**, 3276-3282.
13 Zhuang, X. D.; Chen, Y.; Liu, G.; Zhang, B.; Neoh, K. G.; Kang, E.-T.; Zhu, C. X.; Li, Y. X.; Niu, L. J. *Adv. Funct. Mater.* 2010, **20**, 2916-2922.
14 Bandyopadhyay, A.; Sahu, S.; Higuchi, M. *J. Am. Chem. Soc.* 2011, **133**, 1168-1171.
15 Ko, Y. G.; Kwon, W.; Yen, H. J.; Chang, C. W.; Kim, D. M.; Kim, K.; Hahm, S. G.; Lee, T. J.; Liou, G. S.; Ree, M. *Macromolecules*, 2012, **45**, 3749-3758.
16 Wang, K. L.; Liu, Y. L.; Lee, J. W.; Neoh, K. G.; Kang, E. T. *Macromolecules*, 2010, **43**, 7159-7164.
17 Hsu, J. C.; Chen, Y. G.; Kakuchi, T.; Chen, W. C. *Macromolecules.* **2011**, 44, 5168-5177.
18 Yang, Y.; Ouyang, J.; Ma, L.; Tseng, R. J. H.; Chu, C. W. *Adv. Funct. Mater.* 2006, **16**, 1001-1014.
19 Kim, D. M.; park, S.; Lee, T. J.; Hahm, S. G.; Kim, K.; Kim, J. C.; Kwon, W.; Ree, M. *Langmuir*, 2009, **25**, 11713-11719.
20 Liu, S. J.; Wang, P.; Zhao, Q.; Yang, H. Y.; Wong, J.; Sun, H. B.; Dong, X. C.; Lin, W. P.; Huang, W. *Adv. Mater.* 2012, **24**, 2901-2905.

21 Zhuang, H.; Zhou, Q. H.; Li, Y.; Zhang, Q. J.; Li, H.; Xu, Q. F.; Li, N. J.; Lu, J. M. and Wang, L. H. *ACS Appl. Mater. Interfaces.* 2014, **6**, 94-100.
22 Zhang, Y. H.; Zhuang, H.; Yang, Yong.; Xu, X. F.; Bao, Q.; Li, N. J.; Li, H.; Xu, Q. F.; Lu, J. M. and Wang, L. H. *J. Phys. Chem. C.* 2012, **116**, 22832-22839.
23 Hu, B.; Wang, C.; Wang, J.; Gao, J.; Wang, K.; Wu, J.; Zhang, G.; Cheng, W.; Venkateswarlu, B.; Wang, M.; Leea P. S. and Zhang, Q. *Chem. Sci*. 2014, **5**, 3404-3408
24 Fang, L. J.; Chen, S. J.; Zhang, Y. and Zhang, H. Q. *J. Mater. Chem.* 2011, **21**, 2320-2329.
25 Liu, Y. Q. *Acta Crystallogr. Sect. E*. 2007, **63**, m2997-m3006.
26 Wu, H.; Liu, Y.; Li, M.; Chong, Y.; Zeng, M.; Lo, Y. M. and Yin, J. J. *Nanoscale*, 2015, **7**, 4505-4513.
27 Liu, L.; Rui, L.; Gao, Y. and Zhang, W. *Polym. Chem.* 2015, **6**, 1817-1829.
28 Li, H.; Xu, Q. F.; Li, N. J.; Sun, R.; Ge, J. F.; Lu, J. M.; Gu, H. G.; Yan, F. *J. AM. CHEM. SOC.* 2010, **132**, 5542-5543.
29 Liu,Y. Q.; *Acta Crystallogr. Sect. E*. 2007, **63**, 2996-2997.
30 Lim, S. L.; Li, N. J.; Lu, J. M.; Ling, Q. D.; Zhu, C. X.; Kang, E. T.; Neoh, K. G. *ACS Appl. Mater. Interfaces.* 2009, **1**, 60-71.